

Encoding and Decoding with Partitioned Complementary Sequences for Low-PAPR OFDM

Alphan Şahin

Abstract—In this study, we propose partitioned complementary sequences (CSs) where the gaps between the clusters encode information bits to achieve low peak-to-average-power ratio (PAPR) orthogonal frequency division multiplexing (OFDM) symbols. We show that the partitioning rule without losing the feature of being a CS coincides with the non-squashing partitions of a positive integer and leads to a symmetric separation of clusters. We analytically derive the number of partitioned CSs for given bandwidth and a minimum distance constraint and obtain the corresponding recursive methods for enumerating the values of separations. We show that partitioning can increase the spectral efficiency (SE) without changing the alphabet of the non-zero elements of the CS, i.e., standard CSs relying on Reed-Muller (RM) code. We also develop an encoder for partitioned CSs and a maximum-likelihood-based recursive decoder for additive white Gaussian noise (AWGN) and fading channels. Our results indicate that the partitioned CSs under a minimum distance constraint can perform similar to the standard CSs in terms of average block error rate (BLER) and provide a higher SE at the expense of a limited signal-to-noise ratio (SNR) loss.

Index Terms—Complementary sequences, integer compositions, non-squashing partitions, peak-to-average-power ratio, Reed-Muller code.

I. INTRODUCTION

High peak-to-average-power ratio (PAPR) is a long-lasting problem of an orthogonal frequency division multiplexing (OFDM) transmission. Among many other PAPR mitigation methods [1], [2], complementary sequences (CSs), introduced by Marcel Golay [3], allow one to limit the peak instantaneous power of OFDM signals without any optimization method [4]. In [5], Davis and Jedwab showed that $m!/2 \cdot 2^{h(m+1)}$ CSs of length 2^m for $h \in \mathbb{Z}^+$ occur as the elements of the cosets of the first-order Reed-Muller (RM) code within the second-order RM code. Hence, they obtained a notable coding scheme guaranteeing a low PAPR for OFDM symbols while providing good error correction capability. The set of CSs based on Davis and Jedwab's construction is often referred to as *Golay-Davis-Jedwab (GDJ)* sequences or *standard CSs*.

One drawback of the code proposed in [5] is the low spectral efficiency (SE). To address this issue, one direction is to obtain CSs that cannot be generated through the method in [5], i.e., *non-standard* sequences. In [6], it was shown that some Boolean functions containing third-order monomials can lead to CSs. Another direction is to synthesize CSs where their elements belong to a larger alphabet such as quadrature amplitude modulation (QAM) constellation. Li showed that there exist at least $[(m+1)4^{2(q-1)} - (m+1)4^{(q-1)} + 2^{q-1}](m!/2)4^{(m+1)}$

CSs with 4^q -QAM alphabet [7], which generalizes the results in earlier work in [8]–[13] by using a method called *offset method*. In [14], QAM CSs were synthesized by indexing the elements of the unitary matrices and using the properties of Gaussian integers. Another approach that has recently attracted significant interest is to construct complementary sequence sets (CSSs) or complete complementary code as discussed in [15]–[17] and the references therein, which relax the maximum peak instantaneous power of CSs, but are useful to obtain many sequences with large zero-correlation zones. Although the aforementioned constructions are remarkable, they often do not reveal the encoding and decoding procedures. In [18], a CS construction that utilizes different pseudo-Boolean functions for the magnitude and phase of the elements of the synthesized CS, the support, and the seed Golay complementary pair (GCP) was proposed. Since this construction generalizes Davis and Jedwab's method through independently configurable functions, it allows one to develop an encoder and a decoder for CSs while enabling CSs with zero-valued elements and CSs with uniform and non-uniform constellations. This construction was used to develop a neural-network-based encoder and a decoder in [19] and a low-PAPR multi-user scheme in the uplink for the interlaced allocation in 3GPP Fifth Generation (5G) NR operation in unlicensed bands (NR-U) [20].

Developing a low-PAPR encoder based on CSs is not a straightforward task since a set of different CSs is typically constrained in terms of size, sequence length, and alphabet. For example, CSs with a high-order modulation can alter the mean OFDM symbol power and cause a PAPR larger than 3 dB when the entire transmission is considered for the average power calculation. Although it is possible to address this issue by constraining the magnitude of the elements of CSs as done in [18], this issue increases the design complexity and decreases the number of different CSs. The performance of CSs with a high-order modulation can also be worse than the one for CSs with a phase shift keying (PSK) alphabet, e.g., standard sequences, since a high-order modulation often decreases the minimum Euclidean distance of the set of CSs. It is also challenging to enumerate CSs with an arbitrary length. For example, if the degrees-of-freedom (DoF) are different from a typical CS length, i.e., 2^m , the available DoF are not fully exploited to increase the data rate or reduce the error rate. In this study, we aim to address these problems by partitioning the standard CSs based on the information bits by using the theoretical framework in [18], and use CSs with zero-valued elements. It is worth noting that the CSs with zero-valued elements are known in the literature. However,

they are primarily used to address resource allocation in an OFDM symbol as in [18], [20], and [21]. In [22], the CSSs with zero elements are generated through an iterative method with the motivation of cognitive radio applications. To the best of our knowledge, the systematic design of the zero-valued elements of a CS to transmit extra information bits has not been discussed in the literature.

The proposed concept is inherently related to the index modulation (IM). IM is a subclass of permutation modulation [23] and allows one to encode information in the order of discrete objects. Turning on and off the antennas for transmitting extra information, i.e., spatial modulation [24], adjusting the on/off status of available RF mirrors and encoding information on the antenna pattern, i.e., media-based modulation [25], activating/deactivating OFDM subcarriers with modulation symbols, i.e., OFDM with IM (OFDM-IM) [26], are a few examples of the many variants of IM. In [27], extra information bits were transmitted by exploiting the gap between the active subcarriers in each sub-block of OFDM-IM. However, the gaps are not tied to a special structure and associated encoding/decoding operations based on structured gaps are not discussed. Since OFDM-IM is also based on OFDM, it also suffers from high PAPR. In [28], circular-time shifts are applied to OFDM-IM to reduce the PAPR for multiple antennas. In [29] and [30], the dither signals are considered to reduce the PAPR of OFDM-IM symbols by using convex optimization techniques. In [31] and [32], a single-carrier waveform with IM (SC-IM) is investigated for achieving a low PAPR transmission, which eliminates data-dependent optimization techniques. It was shown that the IM can slightly degrade the PAPR benefit of a typical single-carrier (SC) transmission with low-order modulations. This is expected as IM increases the zero crossings in the time domain for SC. In the extreme cases where there is a large DoF for indices with a few index choices, the PAPR of SC-IM symbols can even be worse than that of OFDM-IM due to pulses in an SC scheme [33]. To the best of our knowledge, CSs have not been systematically investigated from the IM perspective in the literature.

A. Contributions and Organization

Comprehensive analysis of partitioned CSs: We analytically derive the number of partitioned CSs for a given bandwidth. We show that the number of CSs increases by a large factor when the partitioning is taken into account and the alphabet of the non-zero elements of the CS remains the same. We also derive the algorithms that map a natural number to the separations between the clusters or vice versa, which are needed for an encoder and a decoder based on partitioned CSs.

Partitioning under a minimum distance constraint: To obtain the partitioned CSs under a minimum Euclidean distance constraint, we propose a partitioning strategy based on the symmetric structure of the partitioned CSs. For a given minimum distance, we derive the cardinality of the partitioned CSs and the algorithms that construct a bijective mapping between a natural number and the separations between the

clusters. We show that partitioned CSs can maintain the distance properties of the standard CSs while offering a similar SE and a better flexibility in bandwidth.

Encoder/decoder for partitioned CSs: We develop an encoder and a recursive decoder for partitioned CSs and compare the partitioned CSs with the standard CSs and polar code in various configurations.

The rest of the paper is organized as follows. In Section II, preliminary discussions on CSs and notations are provided. In Section III, partitioning for CSs is investigated. The cardinality of the partitioned CSs under a minimum distance constraint and the algorithms for enumerating the partitions are discussed. In Section IV, we use the partitioned CSs to obtain low-PAPR OFDM symbols and present the associated encoder and decoder. In Section V, we evaluate the encoder and decoder and compare partitioned CSs with the standard CSs and polar code. We conclude the paper in Section VI with final remarks.

Notation: The sets of complex numbers, real numbers, integers, non-negative integers, positive integers (i.e., natural numbers), and integers modulo H are denoted by \mathbb{C} , \mathbb{R} , \mathbb{Z} , \mathbb{Z}_0^+ , \mathbb{Z}^+ , and \mathbb{Z}_H , respectively. The set of m -dimensional integers where each element is in \mathbb{Z}_H is denoted by \mathbb{Z}_H^m . The assignment operation is denoted by \leftarrow . The constant j is $\sqrt{-1}$.

II. PRELIMINARIES AND DEFINITIONS

A. Sequences, OFDM, and PMEPR

Let $\mathbf{a} = (a_i)_{i=0}^{L-1} \triangleq (a_0, a_1, \dots, a_{L-1})$ be a sequence of length L , where $a_i \in \mathbb{C}$ and $a_{L-1} \neq 0$. We associate the sequence \mathbf{a} with the polynomial $A(z) = a_{L-1}z^{L-1} + a_{L-2}z^{L-2} + \dots + a_0$ in indeterminate z . The aperiodic autocorrelation function (AACF) of the sequence \mathbf{a} is defined as

$$\rho_a(k) \triangleq \begin{cases} \sum_{i=0}^{L-k-1} a_i^* a_{i+k}, & 0 \leq k \leq L-1 \\ \sum_{i=0}^{L+k-1} a_i a_{i-k}^*, & -L+1 \leq k < 0 \\ 0, & \text{otherwise} \end{cases} \quad (1)$$

We express the continuous-time baseband OFDM symbol generated from the sequence \mathbf{a} as $s_a(t) = \sum_{i=0}^{L-1} a_i e^{j2\pi i \frac{t}{T_s}}$ for $t \in [0, T_s)$, where T_s is the symbol duration. The instantaneous envelope power of the baseband OFDM symbol can be examined by evaluating the polynomial $A(z)$ at $|z| = 1$ since $s_a(t) = A(e^{j\frac{2\pi t}{T_s}})$.

In this study, the peak-to-mean-envelope-power ratio (PMEPR) of an admissible sequence $\mathbf{c} \in \mathbb{C}^L$ in a code is defined as $\max_{t \in [0, T_s)} |s_c(t)|^2 / P_{\text{tx}}$, where $P_{\text{tx}} = \mathbb{E}_c[\rho_c(0)]$ is a constant that depends on the code. Note that PAPR measures the peakness of the signal at the analog front-end as $\max_{t \in [0, T_s)} \Re\{s_c(t)e^{2\pi f_c t}\}^2 / P_{\text{tx}}$, where f_c is the carrier frequency [34]. As the PMEPR is an upper bound for the PAPR and its calculation is easier than PAPR, we use PMEPR to quantify the peakness of the signals in this study.

B. Sequence Synthesis

Let f be a function that maps from $\mathbb{Z}_2^m = \{(x_1, x_2, \dots, x_m) | x_j \in \mathbb{Z}_2\}$ to \mathbb{Z}_H , where H is an integer.

The function f can be expressed as a linear combination of the monomials over \mathbb{Z}_H , i.e.,

$$f(\mathbf{x}) = \sum_{k=0}^{2^m-1} c_k \prod_{j=1}^m x_j^{k_j} = c_0 1 + \dots + c_{2^m-1} x_1 x_2 \dots x_m, \quad (2)$$

where $\mathbf{x} \triangleq (x_1, x_2, \dots, x_m)$ and $c_k \in \mathbb{Z}_H$ for $k = \sum_{j=1}^m k_j 2^{m-j}$ and $k_j \in \mathbb{Z}_2$ (i.e., the coefficient of $(k+1)$ th monomial $x_1^{k_1} x_2^{k_2} \dots x_m^{k_m}$ belongs to \mathbb{Z}_H). If the monomial coefficients are in \mathbb{Z}_0^+ , the co-domain of the function f is \mathbb{Z}_0^+ . In this study, \check{f} is defined as $\check{f}(i) \triangleq f \circ e^{-1}(i)$, where $i = e(\mathbf{x}) \triangleq \sum_{j=1}^m x_j 2^{m-j}$. In other words, $\check{f}(i) = f(\mathbf{x})$, where i is the decimal representation of the binary number constructed using all elements in the sequence \mathbf{x} , where x_1 is the most significant bit.

Let $f_i : \mathbb{Z}_2^m \rightarrow \mathbb{Z}_H$ and $f_s : \mathbb{Z}_2^m \rightarrow \mathbb{Z}_0^+$. We synthesize a unimodular complex sequence $\mathbf{a} = (a_i)_{i=0}^{2^m-1}$ by listing the values of $a_i = \xi^{j\check{f}_i(i)}$ for $\xi \triangleq e^{\frac{2\pi}{H}}$. By modifying the polynomial associated with the sequence \mathbf{a} , we generate a new sequence $\mathbf{c} = (c_i)_{i=0}^{L-1}$ with zero elements as

$$C(z) = \sum_{i=0}^{L-1} c_i z^i = \sum_{i=0}^{2^m-1} a_i z^{\check{f}_s(i)+i},$$

for $L \geq 2^m$.

In this study, we define the support of the sequence \mathbf{c} as $\text{supp}(\mathbf{c}) \triangleq \{i \in \mathbb{Z}_L | c_i \neq 0\}$.

C. Complementary Sequences

The sequence pair (\mathbf{a}, \mathbf{b}) is a GCP if $\rho_a(k) + \rho_b(k) = 0$ for $k \neq 0$ and the sequences \mathbf{a} and \mathbf{b} are referred to as CSs. In this study, we use a specific CS construction that leads to CSs with zero elements, based on Theorem 2 discussed in [18]:

Theorem 1 ([18]). *Let $\boldsymbol{\pi} = (\pi_n)_{n=1}^m$ be a sequence defined by a permutation of $\{1, 2, \dots, m\}$. For any $d', d_n \in \mathbb{Z}_0^+$, $H \in \mathbb{Z}^+$, and $k_n, k' \in \mathbb{Z}_H$ for $n = 1, 2, \dots, m$, let*

$$f_i(\mathbf{x}) = \frac{H}{2} \sum_{n=1}^{m-1} x_{\pi_n} x_{\pi_{n+1}} + \sum_{n=1}^m k_n x_{\pi_n} + k', \quad (3)$$

$$f_s(\mathbf{x}) = \sum_{n=1}^m d_n x_n + d'. \quad (4)$$

Then, the sequence $\mathbf{t} = (t_i)_{i=0}^{L-1}$, where its associated polynomial is given by

$$T(z) = \sum_{i=0}^{2^m-1} \xi^{j\check{f}_i(i)} z^{\check{f}_s(i)+i}, \quad (5)$$

is a CS of length $L = 2^m + d' + \sum_{n=1}^m d_n$.

For Theorem 1, we set the polynomials related to the magnitude of the elements of the CS and the seed GCP in [18, Theorem 2] to 1. In addition, we introduce d' that prepends d' zero-valued elements to the synthesized sequence without changing the properties of CSs. We also set the domain of k' and k_n to \mathbb{Z}_H for $n \in \{1, 2, \dots, m\}$, i.e., (3) leads to a second-order RM code with H -PSK alphabet [5].

If $\check{f}_s(i) + i$ and $\check{f}_s(j) + j$ are identical for $i \neq j$, $\xi^{j\check{f}_i(i)}$ and $\xi^{j\check{f}_i(j)}$ are superposed on the $(\check{f}_s(i) + i)$ th element of the sequence. In [18], the conditions given by

$$d_\ell \geq d_{\ell+1} + d_{\ell+2} + \dots + d_m, \quad (6)$$

for $1 \leq \ell \leq m-1$ are proposed to avoid such superpositions. In this study, a CS is called a *non-partitioned CS* if $d_n = 0$ for $n \in \{1, 2, \dots, m\}$. The set of non-partitioned H -PSK CSs based on (3) is referred to as *standard CSs*. If the conditions in (6) hold, the resulting sequences for any $d_1, \dots, d_n \geq 0$ are *partitioned CSs*.

D. Non-squashing Partitions

A partition of a positive integer P into m parts, i.e., $P = p_1 + p_2 + \dots + p_m$, is defined as *non-squashing* [35] if $p_\ell \geq p_{\ell+1} + p_{\ell+2} + \dots + p_m$ holds for $1 \leq \ell \leq m-1$ and $p_n \in \mathbb{Z}^+$ for $n = 1, 2, \dots, m$. The term of non-squashing partition was first coined in [35] for a problem called *box-stacking problem*. Assume that there are m boxes where each box is labeled as $1, 2, \dots, m$. Suppose that the n th box can support a total weight of n grams. How many different ways of putting the boxes in a single stack are there such that no box will be squashed by the weight of the boxes above it? The solution to this problem and a bijective mapping between binary partitions [36] and non-squashing partitions were discussed in [35], which also led to various generalizations on non-squashing partitions [37]–[39].

The condition given in (6) to eliminate the superposition of elements of a CS interestingly coincides with the non-squashing partitions of $P = \sum_{n=1}^m d_n$ into m parts, except that d_n can be equal to zero. Hence, (d_1, d_2, \dots, d_m) can be considered as a sequence where (d_1, d_2, \dots, d_k) is a non-squashing partition of $P = \sum_{n=1}^k d_n \geq 1$ into k parts, $d_n \neq 0$ for $n \in \{1, \dots, k\}$ and $d_{k+1} = \dots = d_m = 0$ for a given $k \in \{1, \dots, m\}$. For $k = 0$, $d_n = 0$ for $n \in \{1, 2, \dots, m\}$.

III. PARTITIONED COMPLEMENTARY SEQUENCES

A. Problem Statement

Consider a baseband OFDM signal $s_t(t)$, where the associated polynomial for the sequence \mathbf{t} is (5). Let M be the number of available subcarriers for $M \geq L \geq 2^m$. Assume that the conditions in (6) hold true. In this case, the number of zero-valued subcarriers in the frequency domain can be quantified as $Z = M - 2^m$ since the number of non-zero elements of the sequence \mathbf{t} is 2^m in Theorem 1. In this study, we exploit the Z zero-valued subcarriers for encoding extra information bits by manipulating the support of the sequence \mathbf{t} with (4), where the non-zero elements of sequence \mathbf{t} are from the standard CSs formed by (3).

In Theorem 1, the support of the sequence \mathbf{t} is determined by the values of d' and d_n for $n \in \{1, 2, \dots, m\}$ based on the function in (4). Hence, in order to maintain the properties of CSs, the partitioning cannot be done arbitrarily. While d' shifts the sequence by prepending zeroes to the sequence, the impact of d_n is governed by the monomial x_n . For example, d_1 causes the last 2^{m-1} elements to be shifted by d_1 as the last 2^{m-1} elements of the corresponding sequence for the monomial x_1 in (4) is 1. For d_2 , two clusters of size 2^{m-2}

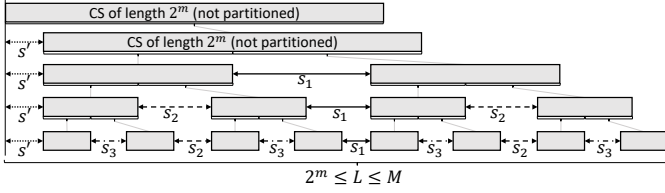


Fig. 1. The support of the CS changes based on the values of s' and s_n for $n = \{1, 2, 3\}$, where the number of zero-valued elements is $s' + s_1 + 2s_2 + 4s_3$. The number of zeroes can be chosen arbitrarily without affecting the properties of a CS since the partitioning follows (4).

are shifted by d_2 since the corresponding sequence for x_2 has two clusters of size 2^{m-2} . Under the condition given in (6), the impact of d' and d_n for $n \in \{1, 2, \dots, m\}$ on the support can be equivalently characterized by the distance between the non-zero clusters. Due to the enumeration of x_1, \dots, x_m in lexicographic order, the support of the sequence \mathbf{t} changes symmetrically as illustrated in Fig. 1. For instance, a standard CS constructed with (3) can be partitioned in two clusters and the distance between the clusters can be arbitrarily chosen as $s_1 \in \mathbb{Z}_0^+$ without losing the features of CSs. Each cluster can also be divided into two sub-clusters equivalently and the distance between two sub-clusters can be controlled by another parameter $s_2 \in \mathbb{Z}_0^+$. The same partitioning process can be continued till the m th step and the amount of separation at the n th step can be analytically expressed as

$$s_n = d_n - \sum_{i=n+1}^m d_i, \quad (7)$$

for $n = 1, 2, \dots, m$, which defines a bijective mapping between (s_1, s_2, \dots, s_m) and (d_1, d_2, \dots, d_m) .

Given $Z = M - 2^m$ zero-valued subcarriers, the first question we need to address is how many different $(d', d_1, d_2, \dots, d_m)$ sequences exist under the condition in (6). The same problem can equivalently be stated as the number of different (s', s_1, \dots, s_m) sequences such that

$$s' + s_1 2^0 + s_2 2^1 + \dots + s_m 2^{m-1} \leq Z, \quad (8)$$

where $s' = d' \in \mathbb{Z}_0^+$ and $s_n \in \mathbb{Z}_0^+$ for $n = 1, 2, \dots, m$. This problem is directly related to the subsequent questions:

- 1) How many extra information bits can be transmitted by changing the support of the synthesized CSs within the M subcarriers in the frequency domain?
- 2) For a given M , how to choose m such that the number of synthesized CSs with partitioning is maximum?
- 3) Can the partitioning maintain the coding gain accomplished for the non-zero elements through the function in (3)?
- 4) What are encoding and decoding procedures if the support of the sequence changes based on information bits?

B. Cardinality Analysis

Let $\mathcal{D}^{(m)}(M, H)$ denotes the number of different partitioned H -PSK CSs based on Theorem 1, where their lengths

are less than or equal to M . It is well-known that the number of H -PSK CSs through the function given in (3) is

$$\mathcal{C}^{(m)}(H) \triangleq \begin{cases} H^{m+1} m! / 2, & m > 0 \\ H, & m = 0 \end{cases}, \quad (9)$$

where H is an even positive integer [5], [40]. Let $\mathcal{B}^{(m)}(Z)$ and $\mathcal{A}^{(m)}(Y)$ be the number of distinct sequences $(s', s_1, s_2, \dots, s_m)$ under the condition in (8) for a given Z and the number of distinct sequences (s_1, s_2, \dots, s_m) such that $\sum_{n=1}^m s_n 2^{n-1} \leq Y \in \mathbb{Z}_0^+$, respectively. $\mathcal{D}^{(m)}(M, H)$ can then be obtained as follows:

Theorem 2. Let $m, Y \in \mathbb{Z}_0^+$ and $H, M \in \mathbb{Z}^+$.

$$\mathcal{D}^{(m)}(M, H) = \mathcal{B}^{(m)}(M - 2^m) \mathcal{C}^{(m)}(H), \quad (10)$$

where

$$\mathcal{B}^{(m)}(Z) = \frac{1}{2} \mathcal{A}^{(m+1)}(2Z + 1), \quad (11)$$

and

$$\mathcal{A}^{(m)}(Y) = \begin{cases} \sum_{i=0}^Y \mathcal{A}^{(m-1)}(\lfloor \frac{i}{2} \rfloor), & m > 1 \\ Y + 1, & m = 1 \end{cases}. \quad (12)$$

Proof. The number of zero-valued elements is $Z = M - 2^m$. Therefore, for a given set of $\{\pi, k_1, \dots, k_n, k'\}$, there exist $\mathcal{B}^{(m)}(M - 2^m)$ distinct sequences for $(s', s_1, s_2, \dots, s_m)$. The parameter s' can range from 0 to Z . Hence, by the definitions of $\mathcal{A}^{(m)}(Y)$ and $\mathcal{B}^{(m)}(Z)$, $\mathcal{B}^{(m)}(Z)$ can be expressed as

$$\mathcal{B}^{(m)}(Z) = \sum_{i=0}^Z \mathcal{A}^{(m)}(Z - i) = \sum_{i=0}^Z \mathcal{A}^{(m)}(i). \quad (13)$$

The condition $\sum_{n=1}^m s_n 2^{n-1} \leq Y$ can be re-written as

$$\sum_{n=2}^m s_n 2^{n-2} \leq \frac{Y - s_1}{2}, \quad (14)$$

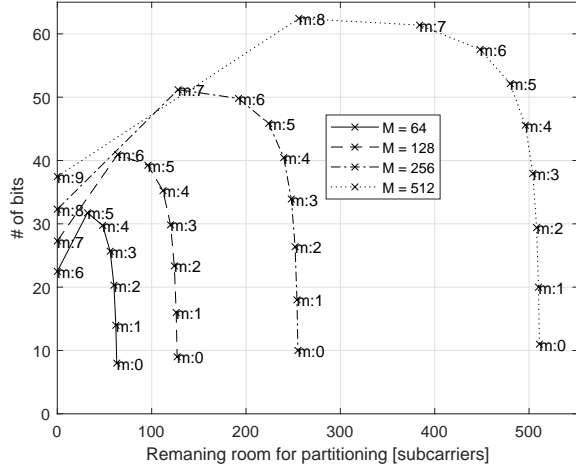
where s_1 can be any integer between 0 and Y . The cardinality of the sequences (s_2, \dots, s_m) under the condition in (14) can be expressed as $\mathcal{A}^{(m-1)}(\lfloor (Y - s_1)/2 \rfloor)$. Therefore,

$$\mathcal{A}^{(m)}(Y) = \sum_{i=0}^Y \mathcal{A}^{(m-1)}\left(\left\lfloor \frac{Y - i}{2} \right\rfloor\right). \quad (15)$$

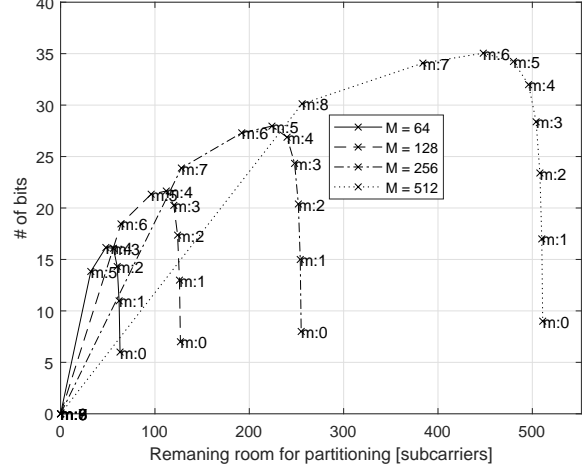
For $m = 1$, $\mathcal{A}^{(1)}(Y) = Y + 1$ since there is only s_1 that can be any integer between 0 and Y . Also, (13) can be re-expressed as

$$\sum_{i=0}^Z \mathcal{A}^{(m)}(i) = \frac{1}{2} \sum_{i=0}^{2Z+1} \mathcal{A}^{(m)}(\lfloor i/2 \rfloor) = \frac{1}{2} \mathcal{A}^{(m+1)}(2Z + 1). \quad \square$$

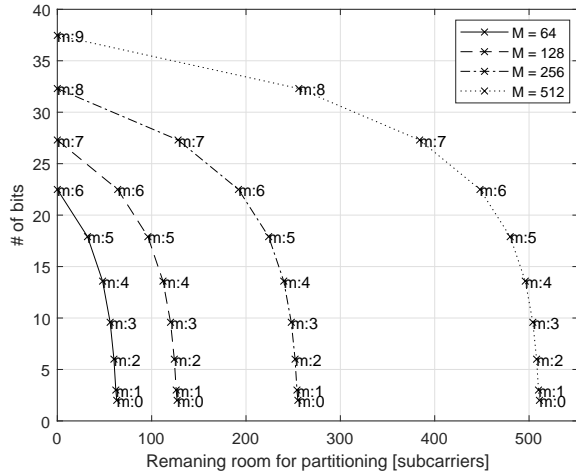
Let n_{total} , n_{supp} , $n_{\text{non-zero}}$, and ρ denote the number of maximum information bits represented by a CS, the number of maximum information bits conveyed by the support of a CS, the number of maximum information bits carried by the non-zero elements of a CS, and the SE, respectively. Based on Theorem 2, n_{total} , n_{supp} , $n_{\text{non-zero}}$, and ρ can be calculated as $n_{\text{total}} = \log_2 \mathcal{D}^{(m)}(M, H)$, $n_{\text{supp}} = \log_2 \mathcal{B}^{(m)}(M - 2^m)$,



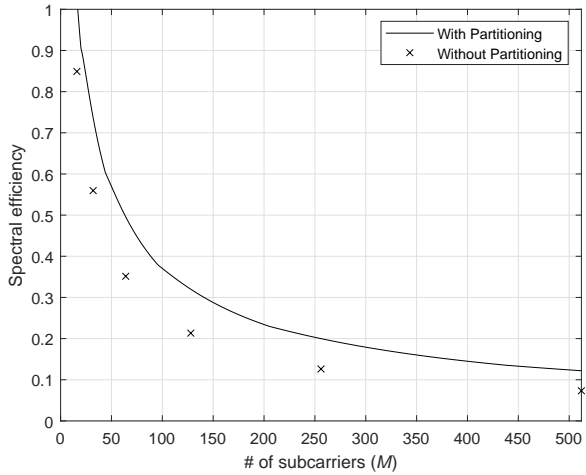
(a) The total number of bits encoded with the non-zero elements and the supports of CSs (n_{total}).



(b) The total number of bits encoded with the supports of CSs (n_{supp}).



(c) The total number of bits encoded with the non-zero elements of CSs ($n_{\text{non-zero}}$).



(d) Maximum achievable SE for a given number of subcarriers.

Fig. 2. Partitioning CSs can increase the number of information bits that can be encoded while increasing the SE as compared to the case without partitioning ($H = 4$).

$n_{\text{non-zero}} = \log_2 \mathcal{C}^{(m)}(H)$, and $\rho = \lfloor \log_2 \mathcal{D}^{(m)}(M, H) \rfloor / M$, respectively.

In Fig. 2, we analyze how n_{total} , n_{supp} , and $n_{\text{non-zero}}$ change for given $M \in \{64, 128, 256, 512\}$ and $m \leq 9$ and provide the maximum achievable SE for a given number of subcarriers $M \in \{16, 17, \dots, 512\}$ for $H = 4$. As shown in Fig. 2(a), the surprising result is that n_{total} is not maximum when all available subcarriers are utilized based on the Davis and Jedwab's encoder in (3). For example, for $M = 512$, n_{total} reaches to 62.43 bits for $m = 8$ and $Z = 256$ while it is 37.47 bits for $m = 9$ and $Z = 0$. In other words, the number of different CSs by using only (3) is improved approximately by a factor of 2^{25} without changing the alphabet of the non-zero elements of the CS (i.e., H -PSK) when the partitioning is taken into account. As shown in Fig. 2(b), n_{supp} first increases by decreasing m as the remaining room for the partitioning increases. However, it sharply decreases after a certain value

of m since the number of clusters (i.e., 2^m) decreases for a smaller m . Fig. 2(c) illustrates how fast $n_{\text{non-zero}}$ decreases with a smaller m . Since n_{supp} increases faster than the degradation of $n_{\text{non-zero}}$ when m decreases (up to a certain value of m), n_{total} improves. This implies that a large number of information bits can be encoded with the partitioned CSs. In Fig. 2(d), we provide the maximum achievable SE with the partitioned CSs for a given number of subcarriers with a computer search. We observe that the maximum SE increases noticeably with the partitioning for a large M as compared to the cases without partitioning. The partitioned CSs also exploit the available subcarriers better than the cases without partitioning as their lengths can be non-power-of-two.

C. Minimum Distance Analysis

Let d_{min} be the minimum Euclidean distance for the set of the partitioned CSs for given m and M , where the non-

zero elements follow Davis and Jedwab's construction. We can obtain d_{\min} as

$$d_{\min} = \min\{d_{\text{non-zero}}, d_{\text{supp}}\}, \quad (16)$$

where $d_{\text{non-zero}}$ and d_{supp} are the minimum Euclidean distances between two different CSs such that they have identical and different supports, respectively.

Assume that $H \triangleq 2^h$ for $h \in \mathbb{Z}^+$, and $m > 0$. In [5], it was shown that the minimum Lee distance of the code based on (3) for $h = 1$ and $h > 1$ are 2^{m-2} and 2^{m-1} , respectively. Hence, for a given support, $d_{\text{non-zero}}$ can be calculated as

$$d_{\text{non-zero}} = \begin{cases} \sqrt{M}, & h = 1 \\ \sqrt{2M} \sin\left(\frac{\pi}{2^h}\right), & h \geq 1 \end{cases}, \quad (17)$$

since the magnitude of each non-zero element is scaled to $r \triangleq \sqrt{M}/2^m$ as we utilize $M \geq 2^m$ subcarriers, where 2^m of them are non-zero and the minimum distance for H -PSK alphabet is $2r \sin\left(\frac{\pi}{H}\right)$.

Lemma 1. *Without any restriction on (s', s_1, \dots, s_m) , d_{supp} is bounded as*

$$d_{\text{supp}} \geq \sqrt{\frac{M}{2^{m-1}}}. \quad (18)$$

Proof. Let \mathbf{t}_1 and \mathbf{t}_2 be two CS with different supports, where $|\text{supp}(\mathbf{t}_1)| = |\text{supp}(\mathbf{t}_2)| = 2^m$. As \mathbf{t}_1 and \mathbf{t}_2 have different supports, $|\text{supp}(\mathbf{t}_1) \cap \text{supp}(\mathbf{t}_2)| \leq 2^m - 2$ must hold. The Euclidean distance between \mathbf{t}_1 and \mathbf{t}_2 is minimum if the elements on the support are identical, leading to $d_{\text{supp}} \geq r\sqrt{2}$. \square

It can also be shown that (18) is tight for same values of m :

Example 1. For $m = 3$, consider the cases where $\{(s', s_1, s_2, s_3) = (0, 0, 0, 0), \boldsymbol{\pi} = (3, 2, 1)\}$ and $\{(s', s_1, s_2, s_3) = (0, 1, 0, 0), \boldsymbol{\pi} = (2, 3, 1)\}$ for $k_n = k' = 0$ for $n = 1, 2, 3$, $H = 4$, and $M = 9$. The corresponding sequences for the former and the latter cases can be obtained as

$$\begin{aligned} &(1, 1, 1, -1, 1, 1, -1, 1, 0), \\ &(1, 1, 1, -1, 0, 1, -1, 1, 1), \end{aligned}$$

respectively. The elements on the fifth and the ninth positions are different while the rest of the elements for any other position are identical. For this example, $d_{\text{non-zero}} = 3$. Hence, $d_{\min} = 1.5$ since $d_{\text{supp}} = 1.5$ and (18) is tight.

For a large m , d_{supp} can be much smaller than $d_{\text{non-zero}}$. To obtain a larger d_{supp} , we restrict the support of an admissible partitioned CS and exploit the fact that both halves of a partitioned sequence CS have identical partitioning as can be seen in Fig. 1. If the minimum distance for one of the halves is $r\sqrt{2^l}$ for $l \in \mathbb{Z}_0^+$, the minimum distance for the complete sequence increases to $r\sqrt{2^{l+1}}$. The problem of obtaining the partitions with the minimum distance of $r\sqrt{2^l}$ for one of the halves is equal to the original problem in Fig. 1, where the sequence length is 2^{m-1} and the room for

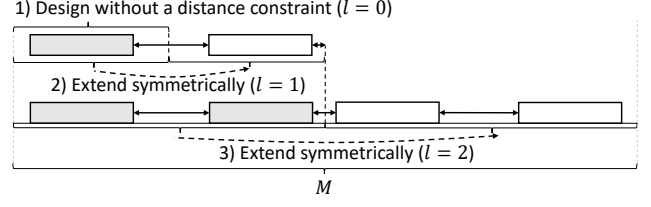


Fig. 3. An example of partitioning with a minimum distance constraint ($l = 2$). If the minimum distance for one of the halves is $r\sqrt{2^l}$, the minimum distance for the complete sequence increases to $r\sqrt{2^{l+1}}$ due to the symmetric support.

partitioning is $\lfloor Z/2 \rfloor$. Thus, the number of different supports where $d_{\text{supp}} \geq r\sqrt{2^{l+1}}$ can be calculated recursively as

$$\mathcal{B}^{(m,l)}(Z) = \mathcal{B}^{(m-1,l-1)}(\lfloor Z/2 \rfloor), \quad (19)$$

where $\mathcal{B}^{(m,0)}(Z) = \mathcal{B}^{(m)}(Z)$. Equation (19) leads to the following conclusion:

Corollary 1. *Let $m, h \in \mathbb{Z}^+$ and $M \geq 2^m$. For $H = 2^h$ and $0 \leq l \leq m - 1$, $\mathcal{D}^{(m,l)}(M, H) = \mathcal{B}^{(m,l)}(M - 2^m) \mathcal{C}^{(m)}(H)$, where $d_{\min} = \min\{d_{\text{non-zero}}, d_{\text{supp}}\}$ and $d_{\text{supp}} \geq \sqrt{M/2^{m-l-1}}$.*

An illustrative example for $l = 2$ is provided in Fig. 3. Since the support of the final CS is restricted to be extended symmetrically in a recursive manner, the minimum distance increases with l .

D. Bijective Mappings

To develop an encoder and a decoder based on the partitioned CSs, the information bits need to be mapped to the sequence (s', s_1, \dots, s_m) or vice versa. Since these mappings are not trivial, we develop the algorithms that map a natural number n to an admissible (s', s_1, \dots, s_m) or vice versa for given Z and l , where $n - 1$ represents the binary number constructed with a set of information bits in decimal. We need the following definitions:

Definition 1. $\epsilon_1(n, Y, m)$ is the function that returns the n th sequence (s_1, \dots, s_m) for a given Y such that $s_1 2^0 + s_2 2^1 + \dots + s_m 2^{m-1} \leq Y$ and $n \in \{1, 2, \dots, \mathcal{A}^{(m)}(Y)\}$.

Definition 2. $\epsilon_2(n, Z, m)$ is the function that returns the n th sequence (s', s_1, \dots, s_m) for a given Z such that $s' + s_1 2^0 + s_2 2^1 + \dots + s_m 2^{m-1} \leq Z$ and $n \in \{1, 2, \dots, \mathcal{B}^{(m)}(Z)\}$.

Definition 3. $\epsilon_3(n, Z, m, l)$ is the function that returns the n th sequence (s', s_1, \dots, s_m) for a given Z such that $s' + s_1 2^0 + s_2 2^1 + \dots + s_m 2^{m-1} \leq Z$ and $d_{\text{supp}} \geq \sqrt{M/2^{m-l-1}}$ and $n \in \{1, 2, \dots, \mathcal{B}^{(m,l)}(Z)\}$.

Definition 4. The inverse functions of $\epsilon_1(n, Y, m)$, $\epsilon_2(n, Z, m)$, and $\epsilon_3(n, Z, m, l)$ are $\epsilon_1^{-1}((s_1, \dots, s_m), Y, m)$, $\epsilon_2^{-1}((s', s_1, \dots, s_m), Z, m)$, and $\epsilon_3^{-1}((s', s_1, \dots, s_m), Z, m, l)$, respectively.

1) *Mapping from natural numbers to separations:* For $l > 0$, the function $\epsilon_3(n, Z, m, l)$ first obtains the sequence (s_1, \dots, s_m) by calling itself as $\epsilon_3(n, \lfloor Z/2 \rfloor, m-1, l-1)$. After

Algorithm 1: Mapping between natural numbers and separations

Function $(s', s_1, \dots, s_m) = \epsilon_3(n, Z, m, l)$

```

if  $l = 0$  then
   $(s', s_1, \dots, s_m) = \epsilon_2(n, Z, m)$ 
else
   $(s_1, \dots, s_m) \leftarrow \epsilon_3(n, \lfloor Z/2 \rfloor, m-1, l-1)$ 
   $s_1 \leftarrow 2s_1$ 
   $s' \leftarrow \lfloor Z/2 \rfloor - (\sum_{i=0}^{m-1} s_{i+1}2^i)/2$ 

```

Function $(s', s_1, \dots, s_m) = \epsilon_2(n, Z, m)$

```

Calculate  $n(c) = \sum_{i=0}^c \mathcal{A}^{(m)}(Z-i) \leq n$  for the largest  $c$ 
 $s' \leftarrow c$ 
 $(s_1, \dots, s_m) \leftarrow \epsilon_1(n-n(c), Z-c, m)$ 

```

Function $(s_1, \dots, s_m) = \epsilon_1(n, Y, m)$

```

if  $m = 1$  then
   $s_1 \leftarrow n-1$ 
else
  Calculate  $n(c) = \sum_{i=0}^c \mathcal{A}^{(m)}(\lfloor (Y-i)/2 \rfloor)$  for the largest  $c$ 
   $s_1 \leftarrow c$ 
   $(s_2, \dots, s_m) = \epsilon_1(n-n(c), \lfloor (Y-c)/2 \rfloor, m-1)$ 

```

Function $n = \epsilon_3^{-1}((s', s_1, \dots, s_m), Z, m, l)$

```

if  $l = 0$  then
   $n = \epsilon_2^{-1}((s', s_1, \dots, s_m), Z, m)$ 
else
   $s_1 \leftarrow s_1/2$ 
   $n \leftarrow \epsilon_3^{-1}((s_1, \dots, s_m), \lfloor Z/2 \rfloor, m-1, l-1)$ 

```

Function $n = \epsilon_2^{-1}((s', s_1, \dots, s_m), Z, m)$

```

Calculate  $n(s') = \sum_{i=0}^{s'-1} \mathcal{A}^{(m)}(Z-i)$ 
 $n = n(s') + \epsilon_1^{-1}((s_1, \dots, s_m), Z-s', m)$ 

```

Function $n = \epsilon_1^{-1}((s_1, \dots, s_m), Y, m)$

```

 $n \leftarrow 1$ 
if  $m = 1$  then
   $n \leftarrow s_1 + 1$ 
else
  Calculate  $n(s_1) = \sum_{i=0}^{s_1-1} \mathcal{A}^{(m-1)}(\lfloor (Y-i)/2 \rfloor)$ 
   $n \leftarrow n(s_1) + \epsilon_1^{-1}((s_2, \dots, s_m), \lfloor (Y-s_1)/2 \rfloor, m-1)$ 

```

setting $s_1 \leftarrow 2s_1$ (due to the symmetric support of the halves), it calculates s' as $s' \leftarrow \lfloor Z/2 \rfloor - (\sum_{i=0}^{m-1} s_{i+1}2^i)/2$. For $l = 0$, the corresponding sequence is calculated with $\epsilon_2(n, Z, m)$ as there is no restriction on the support.

The function $\epsilon_2(n, Z, m)$ utilizes (13). It calculates s' as the largest c such that $n(c) = \sum_{i=0}^c \mathcal{A}^{(m)}(Z-i) \leq n$. Hence, the remaining sequence (s_1, \dots, s_m) can be identified as $(s_1, \dots, s_m) = \epsilon_1(n-n(c), Z-c, m)$.

The function $\epsilon_1(n, Y, m)$ calculates s_1 as the largest c such that $n(c) = \sum_{i=0}^c \mathcal{A}^{(m)}(\lfloor (Y-i)/2 \rfloor) \leq n$ for $m > 1$ based on (15). It obtains the remaining sequence (s_2, \dots, s_m) from $\epsilon_1(n-n(c), \lfloor (Y-c)/2 \rfloor, m-1)$. For $m = 1$, s_1 is $n-1$.

The pseudocodes for $\epsilon_1(n, Y, m)$, $\epsilon_2(n, Z, m)$, and $\epsilon_3(n, Z, m, l)$ are provided in Algorithm 1.

2) *Mapping from separations to natural numbers:*

The function $\epsilon_3^{-1}((s', s_1, \dots, s_m), Z, m, l)$ returns n as $\epsilon_3^{-1}((s_1/2, \dots, s_m), \lfloor Z/2 \rfloor, m-1, l-1)$. For $l = 0$, n is calculated with $\epsilon_2^{-1}((s', s_1, \dots, s_m), Z, m)$.

The function $\epsilon_2^{-1}((s', s_1, \dots, s_m), Z, m)$ calculates how much s' contributes to n as $n(s') = \sum_{i=0}^{s'-1} \mathcal{A}^{(m)}(Z-i)$ by using (13). It obtains n as $n(c) + \epsilon_1^{-1}((s_1, \dots, s_m), Z-s', m)$.

The function $\epsilon_1^{-1}((s_1, \dots, s_m), Y, m)$ calculates the contri-

bution of s_1 as $n(s_1) = \sum_{i=0}^{s_1-1} \mathcal{A}^{(m-1)}(\lfloor (Y-i)/2 \rfloor)$ for $m > 1$ by exploiting (15). It obtains n as $n(c) + \epsilon_1^{-1}((s_2, \dots, s_m), \lfloor (Y-s_1)/2 \rfloor, m-1)$. For $m = 1$, n is s_1+1 . The pseudocodes for $\epsilon_1^{-1}((s_1, \dots, s_m), Y, m)$, $\epsilon_2^{-1}((s', s_1, \dots, s_m), Z, m)$, and $\epsilon_3^{-1}((s', s_1, \dots, s_m), Z, m, l)$ are provided in Algorithm 1.

IV. ENCODER AND DECODER

In this section, we use the partitioned CSs to synthesize low-PAPR OFDM symbols and discuss the corresponding encoding and decoding operations.

A. Encoder

We first split the information bits into two bit sequences that are mapped to (k', k_1, \dots, k_m) and $\{\pi, (s', s_1, \dots, s_m)\}$, i.e., $\mathbf{b}_{\text{non-zero}}$ and $\mathbf{b}_{\pi, \text{supp}}$, respectively. We then convert $\mathbf{b}_{\pi, \text{supp}}$ to a decimal number $i_{\pi, \text{supp}}$. To obtain π and (s', s_1, \dots, s_m) , we decompose $i_{\pi, \text{supp}} = i_{\text{supp}}m!/2 + i_{\pi}$ such that $i_{\pi} < m!/2$ for $i_{\pi}, i_{\text{supp}} \in \mathbb{Z}_0^+$. We then utilize factoradic based on Lehmer code [41] to obtain π from i_{π} . To avoid using π and its reversed version, we assume that $\pi_1 > \pi_m$. We obtain (s', s_1, \dots, s_m) with $\epsilon_3(i_{\text{supp}} + 1, Z, m, l)$ and control the minimum Euclidian distance for the partitioned CSs with l . For (k', k_1, \dots, k_m) , the bit mapping is done based on a Gray mapping, e.g., $00 \rightarrow 0$, $01 \rightarrow 1$, $10 \rightarrow 3$, and $11 \rightarrow 2$ for $H = 4$. After obtaining π , (k', k_1, \dots, k_m) , and (s', s_1, \dots, s_m) , the corresponding baseband OFDM symbol is calculated as $s_t(t)$ where t is a partitioned CS that encodes the information bits. The transmitter diagram is provided in Fig. 4(a). The transmitter maps the elements of a standard CS to the subcarriers chosen based on $\mathbf{b}_{\pi, \text{supp}}$.

B. Decoder

We can express the i th element of the received signal as $r_i = c_i t_i + n_i$, where c_i and n_i are the complex fading channel and the noise coefficients, respectively. Assuming that the channel coefficients are available at the receiver, a maximum-likelihood (ML) decoder corresponds to a minimum distance decoder for additive white Gaussian noise (AWGN), i.e.,

$$\{\hat{\theta}, \hat{\mathbf{s}}\} = \arg \min_{\{\theta, \mathbf{s}\}} \sum_{i=0}^{2^m-1} |c_{I_s(i)} \xi^{j \tilde{f}_i(i; \theta)} - r_{I_s(i)}|^2 \quad (20)$$

$$= \arg \max_{\{\theta, \mathbf{s}\}} \Re \left\{ \sum_{i=0}^{2^m-1} \xi^{-j \tilde{f}_i(i; \theta)} w_{I_s(i)} \right\} - q_s, \quad (21)$$

where $w_{I_s(i)} = c_{I_s(i)}^* r_{I_s(i)}$, $q_s = \sum_{i=0}^{2^m-1} |h_{I_s(i)}|^2$, $\theta = \{\pi, k', k_1, \dots, k_m\}$, $\mathbf{s} = (s', s_1, \dots, s_m)$, and $I_s(i) = i + \tilde{f}_i(i)$.

To solve (21), we consider the principle discussed in [18] and modify it by introducing simplifications due to the PSK alphabet for the non-zero elements of the partitioned CSs. As done in [18], we first decompose $f_i(\mathbf{x}; \theta)$ as $f_i(\mathbf{x}; \theta) = g_i^\ell(\mathbf{x}^\ell; \psi) + x_\ell f_i^\ell(\mathbf{x}^\ell; \phi)$ for $\ell = \{1, 2, \dots, m\}$, where $\mathbf{x}^\ell \triangleq (x_1, x_2, \dots, x_{\ell-1}, x_{\ell+1}, \dots, x_m)$ and $f_i^\ell(\mathbf{x}^\ell) \triangleq \frac{\partial f_i(\mathbf{x})}{\partial x_\ell}$. By using

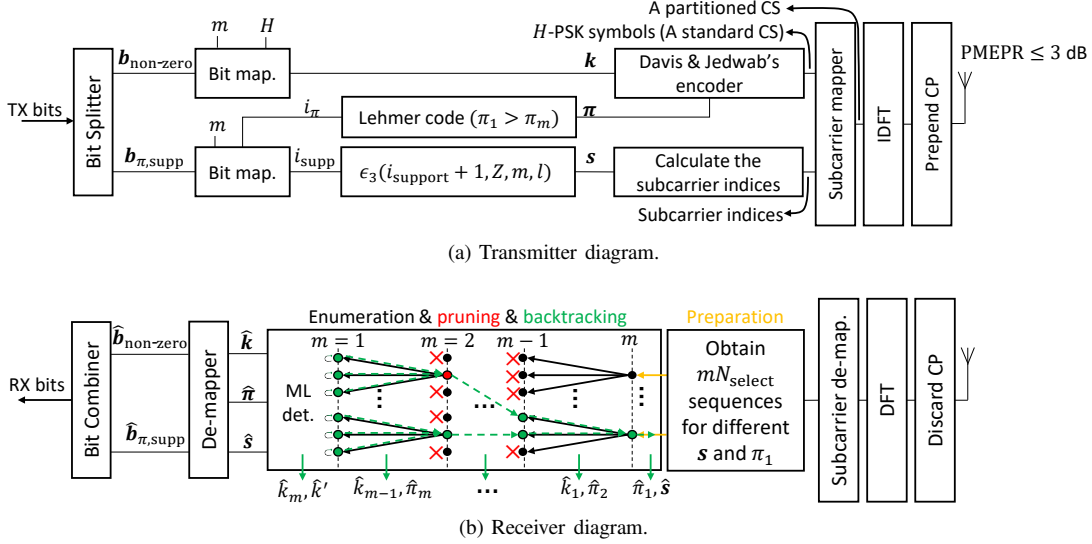


Fig. 4. Transmitter and receiver diagrams for partitioned CSs.

this decomposition, we then re-write the objective function in (21) as

$$\max_{\{\psi, \phi, s\}} \Re \left\{ \sum_{i=0}^{2^m-1} \xi^{-j\tilde{g}_i^\ell(x; \psi)} w_{i, \ell}^\ell \right\} - q_s, \quad (22)$$

where

$$w_i^\ell = w_{I_s(M_\ell(i))} + w_{I_s(M_\ell(i)+2^m-\ell)} \xi^{-j\tilde{f}_i^\ell(i; \phi)}, \quad (23)$$

and $M_\ell(i)$ maps the integers between 0 and 2^m-1 to the values of $\sum_{j=1}^m x_j 2^{m-j}$ in ascending order for $x_\ell = 0$. For $\pi_1 = \ell$, $f_i^\ell(x^\ell)$ can be calculated as $k_1 + \frac{H}{2} x_{\pi_2}$, which leads to $\phi = \{k_1, \pi_2\}$ for a given ℓ . For a hypothesized s , k_1 , π_2 , and ℓ , finding ψ that solves (22) is equivalent to the problem (21), but the length of the sequence $(w_i^\ell)_{i=0}^{2^m-1}$ is 2^m-1 . Hence, by repeating the same procedure, a recursive ML decoder can be obtained. The main bottleneck of this approach is the exponential growth of the enumerated parameters. To address this issue, we terminate the unpromising branches early as done in [18]. As compared to [18], we run the algorithm for the promising values for the sequence s in a parallel. We simplify the decoder by removing steps that are related to high-order constellations. We also reduce the complexity at the backtracking stage as we consider unimodular non-zero elements.

The decoder can be described in the following five stages:

1) *Preparation*: We first choose the most likely $N_{\text{select}} = \min\{\mathcal{B}^{(m, l)}(Z), N_{\text{max}}\}$ separations based on the metric given by

$$\sum_{i=0}^{2^m-1} \max_{c_i \in \mathbb{Z}_H} (\Re\{\xi^{-jc_i} w_i\}) - q_i, \quad (24)$$

i.e., a high signal-to-noise ratio (SNR) estimation of (21), where N_{max} is the maximum number of separations that are considered in the decoding procedure. Since the receiver does not know $\pi_1 \in \{1, 2, \dots, m\}$ in advance, we repeat the selected sequences m times and populate them in \mathbf{W}_m , which leads to

Algorithm 2: A recursive decoder for the partitioned CSs

Function $(\hat{b}_{\text{non-zero}}, \hat{b}_{\pi, \text{supp}}) = \text{main}((c_i)_{i=0}^{M-1}, (r_i)_{i=0}^{M-1}, m, H, Z, l)$
 Calculate $w_i \leftarrow c_i^* r_i$ and $h_i \leftarrow |c_i|^2 / 2$
 Populate \mathbf{W}_m , \mathbf{q}_m , and \mathbf{l}_m for different s and π_1
 Run $(\hat{n}_m, \hat{\pi}, \hat{k}_1, \dots, \hat{k}_m, \hat{k}') = \text{dec}(\mathbf{W}_m, \mathbf{q}_m, \mathbf{l}_m)$
 Obtain s based on \hat{n}_m
 Calculate i_π from $\hat{\pi}$ (permutation to integer)
 Calculate $i_{\text{supp}} = \epsilon_3^{-1}(s, Z, m, l) - 1$
 Calculate $i_{\pi, \text{supp}} = i_{\text{supp}} m! / 2 + i_\pi$
 Calculate $\hat{b}_{\text{non-zero}}$ from $(\hat{k}_1, \dots, \hat{k}_m, \hat{k}')$
 Calculate $\hat{b}_{\pi, \text{supp}}$ from $i_{\pi, \text{supp}}$

Function $(\hat{n}_m, \hat{\pi}, \hat{k}_1, \dots, \hat{k}_m, \hat{k}') = \text{dec}(\mathbf{W}_m, \mathbf{q}_m, \mathbf{l}_m)$
 Enumerate $\mathbf{W}_{m-1}, \mathbf{q}_{m-1}$, and \mathbf{l}_{m-1}
if $m = 1$ **then**
 Set \hat{n}_m as the index of the best sequence in \mathbf{W}_{m-1}
 Obtain \hat{k}' and \hat{k}_1 based on ML detection for \hat{n}_m th sequence
 Set $\hat{\pi} = (1)$
else
 Prune $\mathbf{W}_{m-1}, \mathbf{q}_{m-1}, \mathbf{l}_{m-1}$
 Populate the indices of the chosen sequences in \mathbf{n}_{m-1}
 Run $(i, \pi', \hat{k}_2, \dots, \hat{k}_m, \hat{k}') = \text{dec}(\mathbf{W}_{m-1}, \mathbf{q}_{m-1}, \mathbf{l}_{m-1})$
 Calculate \hat{n}_{m-1} as the i th element of \mathbf{n}_{m-1}
 Calculate \hat{n}_m from \hat{n}_{m-1} (based on the enumeration order)
 Calculate $\hat{\pi}_1$ as the \hat{n}_m th element of \mathbf{l}_{m-1}
 Set $(\hat{\pi}_2, \dots, \hat{\pi}_m)$ as $(1, \dots, \hat{\pi}_1 - 1, \hat{\pi}_1 + 1, \dots, m)_{\pi'}$
 Calculate \hat{k}_1 from \hat{n}_m (based on the enumeration order)

$N = mN_{\text{select}}$ sequences. The corresponding channel quality information and the hypothesized π_1 are listed in \mathbf{q}_m and \mathbf{l}_m , respectively.

2) *Enumeration*: The decoder enumerates $(w_i^\ell)_{i=0}^{2^m-1}$ based on (23) for $m-1$ and H options for π_2 and k_1 , respectively. It then populates the resulting sequences in \mathbf{W}_{m-1} . It also keeps the channel quality information and chosen π_2 in \mathbf{q}_{m-1} and \mathbf{l}_{m-1} , respectively.

3) *Pruning*: To avoid exponential growth, the decoder prunes \mathbf{W}_{m-1} (and the corresponding elements of \mathbf{q}_{m-1} and \mathbf{l}_{m-1}). To this end, it calculates the score given by

$$\sum_{i=0}^{2^m-1} \max_{c_i \in \mathbb{Z}_H} (\Re\{\xi^{-jc_i} w_i'\}) - q_i, \quad (25)$$

for $w'_i \in \mathbf{W}_{m-1}$. The detector then chooses N_{best} sequences based on the score and terminates others. For backtracking, it also lists the indices of the chosen sequences in \mathbf{n}_{m-1} . It then calls itself. It repeats the enumeration and pruning stages till it reaches to $m = 1$.

4) *Backtracking*: For $m = 1$, the decoder performs ML detection for the sequences in \mathbf{W}_{m-1} and finds the \hat{n}_m th sequence in \mathbf{W}_{m-1} that maximizes the likelihood. It then returns the sequence index \hat{n}_m and the detected parameters \hat{k}_1, \hat{k}' , and $\hat{\pi} = (1)$. For $m \geq 2$, the decoder first identifies the chosen sequence by using \mathbf{n}_{m-1} and the provided index from the preceding step, i.e., \hat{n}_{m-1} . It then calculates \hat{k}_1 and $\hat{\pi}_1$ by using \mathbf{l}_{m-1} and \hat{n}_{m-1} and combines them with the detected permutation and the phases from the preceding step.

5) *De-mapping*: After backtracking is finalized, the detected $\hat{\mathbf{s}}$ can be obtained from \hat{n}_m . The parameter \hat{i}_{supp} can then be calculated as $\hat{i}_{\text{supp}} = \epsilon_3^{-1}(\hat{\mathbf{s}}, Z, m, l) - 1$. Therefore, $\hat{i}_{\pi, \text{supp}}$ can be obtained as $\hat{i}_{\pi, \text{supp}} = \hat{i}_{\text{supp}} m! / 2 + \hat{i}_{\pi}$, where \hat{i}_{π} is the corresponding integer for $\hat{\pi}$. It is worth noting that if the detected $\hat{\pi}_1$ is less than the detected $\hat{\pi}_m$, the detector reverses the elements of π and the detected (k_1, \dots, k_m) . Finally, the decoder converts the decimal $\hat{i}_{\pi, \text{supp}}$ and the sequence $(\hat{k}_1, \dots, \hat{k}_m, \hat{k}')$ to $\hat{\mathbf{b}}_{\pi, \text{supp}}$ and $\hat{\mathbf{b}}_{\text{non-zero}}$, respectively. The pseudocode for the decoder is given in Algorithm 2. The receiver diagram is also provided in Fig. 4(b).

C. Complexity

At the preparation stage, the identification of N_{select} best candidates for the separations based on (24) requires the calculation of (24) by $\mathcal{B}^{(m,l)}(Z)$ times and an algorithm for identifying at most N_{max} candidates. The time complexity for (24) increases linearly with 2^m , $\mathcal{B}^{(m,l)}(Z)$, and H and it is larger than the time complexity of the sorting algorithm. Therefore, the time complexity of the preparation stage is $\mathcal{O}(2^m H \mathcal{B}^{(m,l)}(Z))$. It is worth noting that identifying the indices based on sorted subcarrier energy levels can substantially reduce to $\mathcal{O}(2^m H)$. However, since a single misidentified index causes an *ordering* problem (i.e., the decoder needs to deal with not only noise but also permuted and/or erased elements), the decoder with such simplifications tends to work only at high SNR.

At the enumeration stage after the preparation, the decoder enumerates $H(m-1)mN_{\text{select}}$ sequences of length 2^{m-1} from mN_{select} sequences of length 2^m based on (23). The corresponding time complexity can be calculated as $\mathcal{O}(2^{m-1} H m N_{\text{select}})$. Based on (25), the decoder then prunes a majority of the enumerated sequences, i.e., at most N_{best} of them survive. The time complexity of (25) can be calculated as $\mathcal{O}(2^{m-1} H m N_{\text{select}})$. For the following steps, the decoder enumerates $H(m-i)N_{\text{best}}$ sequences of length 2^{m-i} at the i th recursion step for $2 \leq i \leq m-1$ and chooses N_{best} sequences. Therefore, the time complexity is $\mathcal{O}(2^{m-i-1} H N_{\text{best}})$ for the i th recursion step.

Based on our trials, we observe that N_{select} often needs to be larger than N_{best} for a large Z . Thus, the first enumeration step is the most expensive part as compared to the following steps in the recursions, which may prohibit the practical implementations for devices with low computational power. Hence,

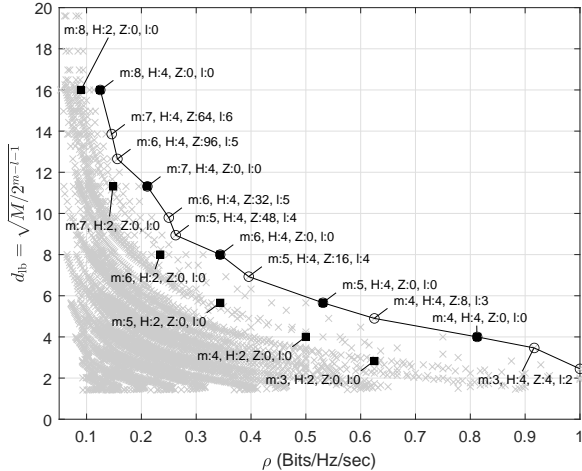
a lower-complexity decoding algorithm for the partitioned CSs is needed and it is currently an open problem.

V. NUMERICAL RESULTS

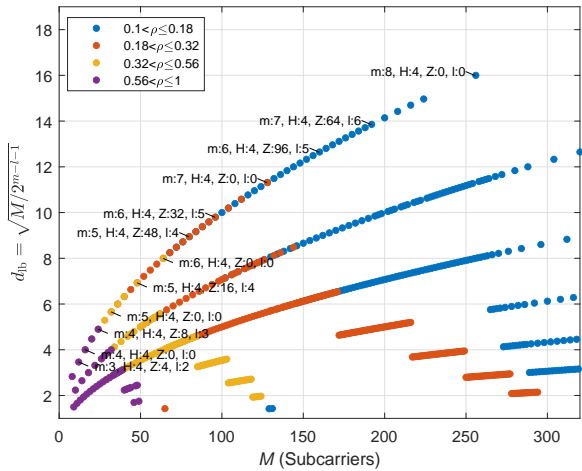
In this section, we evaluate the partitioned CSs for an OFDM-based communication system, numerically. For side-by-side comparisons, we consider the standard CSs proposed in [5] and the polar code in 3GPP 5G New Radio (NR) uplink (UL). For the standard CSs, we consider $m \in \{4, 5, 6, 7\}$. For the partitioned CSs, we also consider the same sequence length as the standard CSs, i.e., $M \in \{16, 32, 64, 128\}$, and set Z as $M/2$ based on Figure 2(a). For the decoder, we set $N_{\text{max}} = 10000$ and $N_{\text{best}} = 400$. The same decoder is used for the standard CSs. For all CSs configurations, we consider OFDM and quadrature phase-shift keying (QPSK), i.e., $H = 4$. For a fair comparison, we adjust the code rate of the polar code such that it leads to the same SE and codeword length as the CSs. We also add 11 cyclic redundancy check (CRC) bits to the information bits and interleave the coded bits. For the decoder, we use a list decoder with soft information, where the list length is set to 64. We use discrete Fourier transform (DFT)-spread OFDM (DFT-s-OFDM) for polar code unless otherwise stated and consider both $\pi/2$ -binary phase-shift keying (BPSK) and $\pi/4$ -QPSK, which are effective to mitigate the PMEPR by reducing the zero-crossings in the time domain. For the multi-path fading channel model, we use ITU Vehicular A with no mobility. We assume that the cyclic prefix (CP) duration is longer than the maximum excess delay of the multi-path channel to avoid inter-symbol interference, the symbol duration is set to $T_s = 66.67 \mu\text{s}$, and the transmitter and receiver are synchronized in both time and frequency.

A. Minimum Distance, Spectral Efficiency, and Bandwidth

In Fig. 5, we evaluate the trade-offs between minimum distance, SE, and bandwidth for partitioned CSs and the standard CSs by calculating these parameters for $m \in \{3, 4, 5, 6, 7, 8\}$, $0 \leq l \leq m-1$, $Z \in \{0, 1, \dots, 256\}$, and $H = \{2, 4\}$. Since $d_{\text{non-zero}} = \sqrt{M}$ for $H = \{2, 4\}$, $d_{\text{min}} \geq d_{\text{lb}} \triangleq \sqrt{M/2^{m-l-1}}$ for $0 \leq l \leq m-1$. In Fig. 5(a), we calculate ρ and d_{lb} for all combinations and mark several best cases that provide the maximum d_{lb} for a given SE. Fig. 5(a) shows that the partitioned CSs support a wide range of SE as opposed to the standard CSs based on (3). We also observe that the partitioned CSs with a smaller m can achieve a similar d_{lb} of the standard CSs. For instance, $d_{\text{lb}} = 8$ for $m = 6$ without partitioning, $d_{\text{lb}} = 8.9$ for $m = 5$, $Z = 48$, and $l = 4$. In Fig. 5(b), we also take the impact of bandwidth on the minimum distance and SE into account. For a given parameter set of SE range and bandwidth, we plot the maximum d_{lb} . For example, when $M = 160$ subcarriers, the $d_{\text{lb}} = 12.65$ is achieved for the configuration $m = 6$, $Z = 96$, and $l = 5$, where the SE is $\rho = 25/160$ bits/Hz/sec, which is between 0.1 and 0.18 bits/Hz/sec. Fig. 5(b) explicitly shows that a larger d_{lb} is achieved for a larger M or a smaller ρ . Although the partitioning does not remedy the loss of SE for a larger M under a minimum distance constraint, it enables many different options for various SEs and bandwidths, which is beneficial for exploiting the available DoF in the frequency domain better.



(a) Minimum distance versus SE.



(b) Minimum distance versus bandwidth for a given range of SE.

Fig. 5. The partitioned CSs can maintain the minimum distance properties of the standard CSs and be compatible with the non-power-two M .

B. PMEPR and Error Rate

In Fig. 6, we provide the PMEPR distributions for various configurations, respectively. As expected, the partitioning maintains the PMEPR benefit of the standard CSs as the partitioned sequences based on Theorem 1 are still CSs. Hence, the maximum PAPR is 3 dB for all configurations of CSs. Since the partitioning does not alter the norm of the sequence, the mean OFDM symbol power also remains constant. The polar code with DFT-s-OFDM is superior to that of OFDM in terms of PMEPR as DFT pre-coding effectively converts the multi-carrier nature of the OFDM to a form of single-carrier waveform. The PMEPR distribution for the polar code with $\pi/2$ -BPSK is better than the one with $\pi/4$ -QPSK. This is expected because the zero-crossings in the time domain are mitigated further with $\pi/2$ -BPSK, as compared to ones with $\pi/4$ -QPSK. Nevertheless, the gap between CSs and the polar code with DFT-s-OFDM with $\pi/2$ -BPSK can still reach up to 3 dB.

In Fig. 7, we provide the BLER versus E_b/N_0 curves in

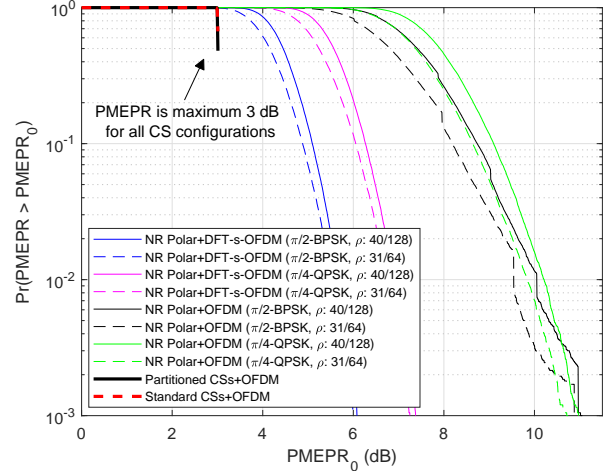
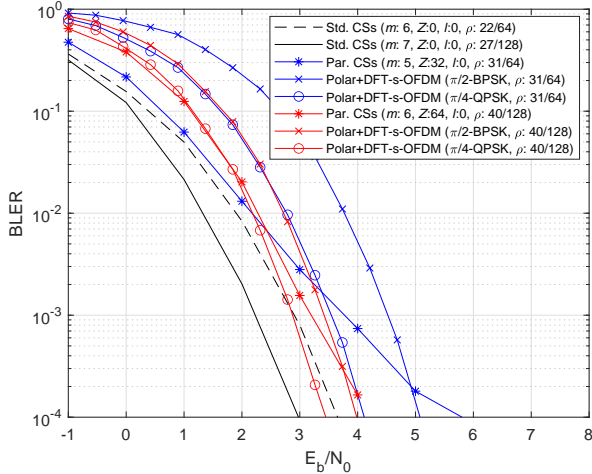


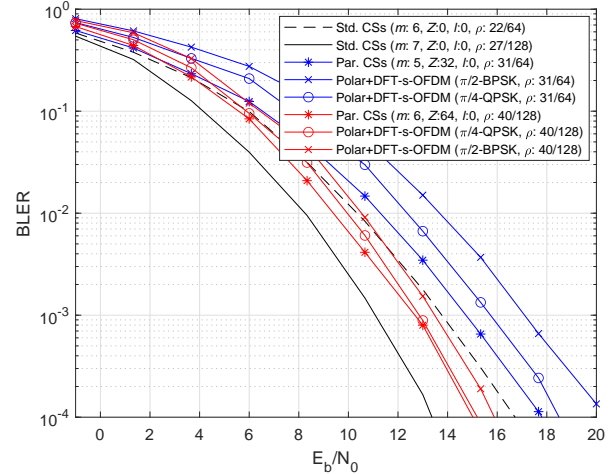
Fig. 6. PMEPR distributions.

AWGN and fading channels. In Fig. 7(a) and Fig. 7(b), we do not restrict the supports of the partitioned CSs, i.e., $l = 0$. As discussed in Section III, under the same bandwidth, the partitioned CSs can yield a higher SE with a smaller m as compared to the standard CSs. For example, $M = 128$, the number of information bits increases to 40 for $m = 6$ whereas it is 27 bits for the standard CSs with $m = 6$. However, since the partitioning decreases the minimum Euclidean distance of the standard CSs, the block error rate (BLER) increases for the partitioned CSs. At $1e-3$ BLER, the losses in E_b/N_0 are approximately 1 dB for both $M = 64$ and $M = 128$, respectively, for the AWGN channel. The slopes of the curves for the standard CSs and the partitioned CSs are also different as the pairwise distance distribution of the set of partitioned CSs is different from the one for the standard CSs. We also observe that the case where $Z = 64$ performs worse than the case where $Z = 32$ for low E_b/N_0 . This is due to the sequence identification at the preparation phase of the decoder, which requires a larger N_{select} for the case where $Z = 64$ at the expense of higher complexity. In the fading channel, the E_b/N_0 losses are approximately 1 dB at $1e-3$ BLER for all cases.

In Fig. 7, we also analyze the error rate with the polar code with $\pi/2$ -BPSK and $\pi/4$ -QPSK under the same spectral efficiency provided by partitioned CSs. As expected, the error rate for the polar code with $\pi/4$ -QPSK is better than the one with $\pi/2$ -BPSK because a larger codeword length is utilized. Nevertheless, the performance of the polar code with $\pi/4$ -QPSK is similar to that of the partitioned CSs. We observe that the performance differences are within the range of 1 dB at $1e-3$ BLER in both AWGN and fading channels. While the polar code has an advantage in terms of receiver complexity as compared to the decoder for the partitioned CS used in this study, the partitioned CS-based encoding is superior to the polar code with $\pi/4$ -QPSK in terms of PMEPR as shown in Fig. 6. Note that the slope of the error rate curves in the fading channel is a function of the bandwidth for all schemes.



(a) AWGN channel.



(b) Fading channel.

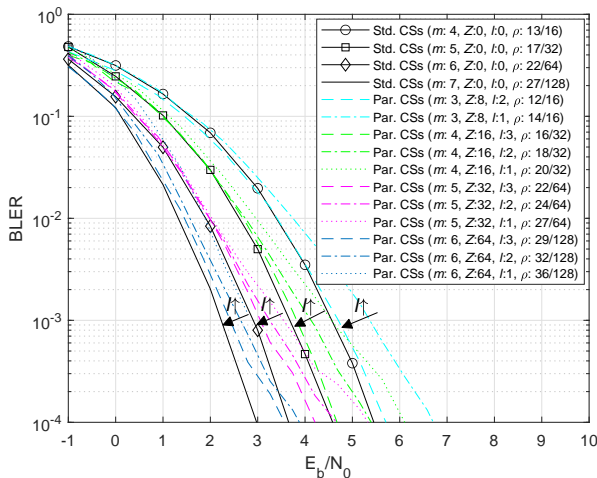
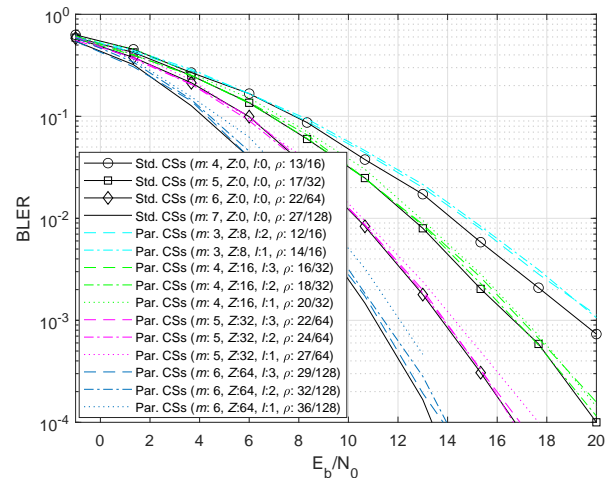
(c) AWGN channel ($l > 0$ for the partitioned CSs).(d) Fading channel ($l > 0$ for the partitioned CSs).

Fig. 7. BLER performance of the partitioned CSs as compared to that of the standard CSs in [5] and polar code with DFT-s-OFDM.

This is because more diversity gain is achieved for a larger M .

In Fig. 7(c) and Fig. 7(d), we consider the cases where the supports of the partitioned CSs are restricted to achieve a larger minimum distance. The E_b/N_0 loss quickly diminishes for all cases with an increasing $l > 0$ in both AWGN and fading channel. For a large l , the partitioned CSs perform similar to the standard CSs with a similar SE. For example, for the case ($m = 6, Z = 64, l = 3$), the SE is 29/128 bits/Hz/sec and it performs similar to the standard CSs, where $m = 7$ and the corresponding SE is 27/128 bits/Hz/sec. The minimum distance for the standard CSs can be calculated as $\sqrt{128}$ when $m = 7$. However, $d_{\min} \geq d_{\text{lb}} = \sqrt{32}$ for the partitioned CSs. The diminishing loss in the average BLER implies that a majority of the pairwise distances for the partitioned CSs are actually larger than $d_{\text{lb}} = \sqrt{32}$. Similar observations can also be made for other cases.

VI. CONCLUSION

In this study, we analyze partitioned CSs for OFDM. We analytically obtain the number of partitioned CSs for given bandwidth and a minimum distance constraint. We derive the corresponding recursive methods for mapping a natural number to a separation and vice versa. We show that the partitioning rule under Theorem 1 has symmetrical characteristics, which can be utilized to restrict the partitions based on a minimum distance constraint. In addition, we develop an encoder and a recursive decoder for partitioned CSs.

Our results indicate that a larger number of CSs can be synthesized as compared to the standard CSs for a given bandwidth through partitioning. For example, for 512 DoF, we show that the number of distinct CSs is increased approximately by a factor of 2^{25} without changing the alphabet of the non-zero elements of the CS (i.e., the standard sequences with H -PSK) with the partitioning. Hence, partitioning provides a way of achieving a larger SE without changing the alphabet of the non-zero elements of the CSs or using a high-

order modulation for CSs. Partitioning without any restriction decreases the minimum Euclidean distance of the standard CSs. By using our encoder and detector, we show that the SNR losses are around 2 dB and 1 dB in AWGN and fading channels at $1e - 3$ BLER, respectively, as compared to the standard CSs. However, under a minimum distance constraint, the partitioned CSs perform similar to the standard CSs in terms of error average BLER and they can utilize the available resources in the frequency domain better than the standard CSs.

The partitioned CSs that we investigate in this paper extend the standard CSs from Davis and Jedwab's encoder in [5] and have some desirable properties such as the adjustable minimum Euclidean distance. To fully exploit the properties of partitioned CSs, a low-complexity decoder is needed, which is currently a difficult open problem. Extending the non-zero elements of partitioned CSs to a larger constellation to increase the minimum distance is also another future research direction that can be pursued. Because of the absence of a tighter SE bound that takes the sequence length, SNR, and PMEPR constraints than the available ones, e.g. [42], [43], in this study, we cannot compare the obtained SE of the proposed scheme with a theoretical bound. Hence, a tight upper bound on the SE is needed for a better understanding of the theoretical limits under PMEPR constraints.

REFERENCES

- [1] G. Wunder, R. F. H. Fischer, H. Boche, S. Litsyn, and J. No, "The PAPR problem in OFDM transmission: New directions for a long-lasting problem," *IEEE Signal Processing Magazine*, vol. 30, no. 6, pp. 130–144, Nov. 2013.
- [2] Y. Rahmatallah and S. Mohan, "Peak-to-average power ratio reduction in OFDM systems: A survey and taxonomy," *IEEE Commun. Surveys Tut.*, vol. 15, no. 4, pp. 1567–1592, Fourth 2013.
- [3] M. Golay, "Complementary series," *IRE Trans. Inf. Theory*, vol. 7, no. 2, pp. 82–87, Apr. 1961.
- [4] B. M. Popovic, "Synthesis of power efficient multitone signals with flat amplitude spectrum," *IEEE Trans. Commun.*, vol. 39, no. 7, pp. 1031–1033, Jul. 1991.
- [5] J. A. Davis and J. Jedwab, "Peak-to-mean power control in OFDM, Golay complementary sequences, and Reed-Muller codes," *IEEE Trans. Inf. Theory*, vol. 45, no. 7, pp. 2397–2417, Nov. 1999.
- [6] Y. Li and Y.-C. Kao, "Structures of non-GDJ golay sequences," in *Proc. International Symposium on Information Theory (ISIT)*, Sep. 2005, pp. 378–381.
- [7] Y. Li, "A construction of general QAM Golay complementary sequences," *IEEE Trans. Inf. Theory*, vol. 56, no. 11, pp. 5765–5771, Nov. 2010.
- [8] C. Rößing and V. Tarokh, "A construction of OFDM 16-QAM sequences having low peak powers," *IEEE Trans. Inf. Theory*, vol. 47, no. 5, pp. 2091–2094, Jul. 2001.
- [9] C. V. Chong and V. Tarokh, "Two constructions of 16-QAM Golay complementary sequences," in *Proc. IEEE International Symposium on Information Theory (ISIT)*, Jun. 2002, p. 240.
- [10] C. V. Chong, R. Venkataramani, and V. Tarokh, "A new construction of 16-QAM Golay complementary sequences," *IEEE Trans. Inf. Theory*, vol. 49, no. 11, pp. 2953–2959, Nov. 2003.
- [11] H. Lee and S. W. Golomb, "A new construction of 64-QAM Golay complementary sequences," *IEEE Trans. Inf. Theory*, vol. 52, no. 4, pp. 1663–1670, Apr. 2006.
- [12] C. Chang, Y. Li, and J. Hirata, "New 64-QAM Golay complementary sequences," *IEEE Trans. Inf. Theory*, vol. 56, no. 5, pp. 2479–2485, May 2010.
- [13] Y. Li, "Comments on 'a new construction of 16-QAM Golay complementary sequences' and extension for 64-QAM Golay sequences," *IEEE Trans. Inf. Theory*, vol. 54, no. 7, pp. 3246–3251, Jul. 2008.
- [14] S. Z. Budišin and P. Spasojević, "Paraunitary-based Boolean generator for QAM complementary sequences of length 2^K ," *IEEE Trans. Inf. Theory*, vol. 64, no. 8, pp. 5938–5956, Aug. 2018.
- [15] C. Chen and S. Wu, "Golay complementary sequence sets with large zero correlation zones," *IEEE Trans. Commun.*, vol. 66, no. 11, pp. 5197–5204, July 2018.
- [16] S. Das, U. Parampalli, S. Majhi, Z. Liu, and S. Budišin, "New optimal Z-complementary code sets based on generalized paraunitary matrices," *IEEE Trans. Signal Process.*, vol. 68, pp. 5546–5558, 2020.
- [17] S. W. Wu, A. Şahin, Z. M. Huang, and C. Y. Chen, "Z-complementary code sets with flexible lengths from generalized Boolean functions," *IEEE Access*, pp. 1–11, Dec. 2020.
- [18] A. Şahin and R. Yang, "A generic complementary sequence construction and associated encoder/decoder design," *IEEE Trans. Commun.*, pp. 1–15, 2021.
- [19] A. Şahin and D. W. Matolak, "Golay layer: Limiting peak-to-average power ratio for OFDM-based autoencoders," in *Proc. IEEE International Conference on Communications (ICC)*, Jun. 2020, pp. 1–7.
- [20] A. Şahin and R. Yang, "An uplink control channel design with complementary sequences for unlicensed bands," *IEEE Trans. Wireless Commun.*, vol. 19, no. 10, pp. 6858–6870, Jul. 2020.
- [21] A. Şahin, X. Wang, H. Lou, and R. Yang, "Low-PAPR multi-channel OOK waveform for IEEE 802.11ba Wake-Up Radio," in *2019 IEEE Global Communications Conference (GLOBECOM)*, Dec. 2019, pp. 1–6.
- [22] Y. Zhou, Y. Yang, Z. Zhou, K. Anand, S. Hu, and Y. L. Guan, "New complementary sets with low PAPR property under spectral null constraints," *IEEE Trans. Inf. Theory*, vol. 66, no. 11, pp. 7022–7032, 2020.
- [23] D. Slepian, "Permutation modulation," *Proceedings of the IEEE*, vol. 53, no. 3, pp. 228–236, Mar. 1965.
- [24] R. Y. Mesleh, H. Haas, S. Sinanovic, C. W. Ahn, and S. Yun, "Spatial modulation," *IEEE Veh. Technol.*, vol. 57, no. 4, pp. 2228–2241, Jul. 2008.
- [25] A. K. Khandani, "Media-based modulation: A new approach to wireless transmission," in *Proc. IEEE International Symposium on Information Theory (ISIT)*, Jul. 2013, pp. 3050–3054.
- [26] E. Başar, Ü. Aygözü, E. Panayircı, and H. V. Poor, "Orthogonal frequency division multiplexing with index modulation," *IEEE Trans. Signal Process.*, vol. 61, no. 22, pp. 5536–5549, Aug. 2013.
- [27] A. Jaradat, J. M. Hamamreh, and H. Arslan, "Orthogonal frequency division multiplexing with subcarrier gap modulation," in *Proc. IEEE International Symposium on Personal, Indoor and Mobile Radio Communications (PIMRC)*, no. Aug., 2020, pp. 1–6.
- [28] A. Vora and K. Kang, "Index modulation with PAPR and beamforming for 5G MIMO-OFDM," in *Proc. IEEE 5G World Forum (5GWF)*, Jul. 2018, pp. 389–394.
- [29] K. Kim, "PAPR reduction in OFDM-IM using multilevel dither signals," *IEEE Commun. Lett.*, vol. 23, no. 2, Jan. 2019.
- [30] J. Zheng and H. Lv, "Peak-to-average power ratio reduction in OFDM index modulation through convex programming," *IEEE Commun. Lett.*, vol. 21, no. 7, pp. 1505–1508, Apr. 2017.
- [31] S. Sugiura, T. Ishihara, and M. Nakao, "State-of-the-art design of index modulation in the space, time, and frequency domains: Benefits and fundamental limitations," *IEEE Access*, vol. 5, pp. 21 774–21 790, Oct. 2017.
- [32] M. Nakao and S. Sugiura, "Dual-mode time-domain single-carrier index modulation with frequency-domain equalization," in *2017 IEEE 86th Vehicular Technology Conference (VTC-Fall)*, 2017, pp. 1–5.
- [33] S. Hoque, C.-Y. Chen, and A. Şahin, "A wideband index modulation with circularly-shifted chirps," in *Proc. IEEE Consumer Commun. & Netw. Conf. (CCNC)*, Jan. 2021, pp. 1–6.
- [34] M. Sharif, M. Gharavi-Alkhansari, and B. H. Khalaj, "On the peak-to-average power of OFDM signals based on oversampling," *IEEE Trans. Commun.*, vol. 51, no. 1, pp. 72–78, Feb. 2003.
- [35] N. Sloane and J. A. Sellers, "On non-squashing partitions," *Discrete Mathematics*, vol. 294, no. 3, pp. 259–274, May 2005.
- [36] M. Hirschhorn and J. Sellers, "A different view of m-ary partitions," *Australasian Journal of Combinatorics*, vol. 30, pp. 193–196, 2004.
- [37] L. H. Sun and M. Zhang, "On the enumeration and congruences for m-ary partitions," *Journal of Number Theory*, vol. 185, pp. 423–433, Apr. 2018.
- [38] A. Folsom, Y. Homma, J. H. Ryu, and B. Tong, "On a general class of non-squashing partitions," *Discrete Mathematics*, vol. 339, no. 5, pp. 1482–1506, May 2016.

- [39] G. E. Andrews and J. A. Sellers, "On Sloane's generalization of non-squashing stacks of boxes," *Discrete Mathematics*, vol. 307, no. 9, pp. 1185–1190, May 2007.
- [40] K. G. Paterson, "Generalized Reed-Muller codes and power control in OFDM modulation," *IEEE Trans. Inf. Theory*, vol. 46, no. 1, pp. 104–120, Jan. 2000.
- [41] D. Lehmer, "Teaching combinatorial tricks to a computer," in *Proc. Sympos. Appl. Math. Combinatorial Analysis Amer. Math. Soc.*, vol. 10, 1960, pp. 179–193.
- [42] K. Paterson and V. Tarokh, "On the existence and construction of good codes with low peak-to-average power ratios," *IEEE Trans. Inf. Theory*, vol. 46, no. 6, pp. 1974–1987, Sep. 2000.
- [43] V. Tarokh and H. Jafarkhani, "On the computation and reduction of the peak-to-average power ratio in multicarrier communications," *IEEE Trans. Commun.*, vol. 48, no. 1, pp. 37–44, Jan. 2000.